7N-89-TM

592190

13P.

SPACE
TELESCOPE
SCIENCE
INSTITUTE

PREPRINT SERIES

No. 346

RELATIVISTIC BEAMING, LUMINOSITY FUNCTIONS, AND THE NUMBER COUNTS OF BL LAC OBJECTS

C. Megan Urry

(NASA-TM-103461) RELATIVISTIC BEAMING, LUMINOSITY FUNCTIONS, AND THE NUMBER COUNTS OF BL LAC OBJECTS (Space Telescope Science Inst.) 13 p

N90-70850

Unclas

00/89 0292190

March 1989

RELATIVISTIC BEAMING, LUMINOSITY FUNCTIONS, AND THE NUMBER COUNTS OF BL LAC OBJECTS

C. Megan Urry

Space Telescope Science Institute

3700 San Martin Drive

Baltimore, Maryland 21218

To be published in the proceedings of

BL Lac Objects: 10 Years After

ed. L. Maraschi

Relativistic Beaming, Luminosity Functions, and the Number Counts of BL Lac Objects

C. Megan Urry

Academic Affairs Division, Space Telescope Science Institute
3700 San Martin Drive, Baltimore, Maryland 21218, U.S.A.

Summary

If specially oriented relativistic jets are a defining characteristic of BL Lac objects as a class, then several consequences follow unavoidably. First, the observed emission is relativistically boosted and may in fact represent only a small fraction of the emitted luminosity of the source. This tends to hide the identity of the "parent population" (those objects with misdirected jets) since intrinsic characteristics may be swamped by the boosted radiation. Second, the parent population must be relatively numerous since only a small fraction of randomly oriented jets would point toward us. In many cases, this has been used in a naïve way to comment on possible parent populations for BL Lac objects (and to argue, erroneously, against the beaming hypothesis). Third — the point stressed in this paper — the observed luminosity distribution of BL Lac objects depends on both the luminosity function (LF) of the parent population and the properties of the jet (its speed and orientation). For simple power-law parent LFs, the shape of the LF for the beamed objects is a distinctive broken power-law which is very flat at low luminosities. For more complicated parent LFs, the beamed LF will still be at least as flat at the low luminosity end.

The flatness of the luminosity function has important consequences for the first two points above and for the beaming theory as a whole: the shape of the luminosity function can be used to confirm or refute the theory, and perhaps to identify the parent population. For flux-limited samples, the different shapes of the parent and beamed LFs must be incorporated in any discussion of the identity of the parent population. Even if the luminosity function cannot be determined accurately because of the lack of complete redshift information (redshifts being, by definition, difficult to measure in BL Lac objects), beaming still predicts that the more readily observable $\log N$-$\log S$ distribution will be very flat, with or without evolution. A qualitative comparison with available estimates of optical and X-ray luminosity functions and number counts of BL Lac objects supports the beaming model.

I. Introduction

No one needs reminding that BL Lac objects are difficult to find. To date, radio and X-ray surveys have discovered the most BL Lacs but their yield is relatively small (see papers by Maccacaro *et al.* and Stocke *et al.*, these proceedings). Optical searches, including a large-area polarization search (see B. Jannuzzi's paper, these proceedings), have been even less successful. In the ten years since the last BL Lac conference, the number of catalogued quasars increased by a factor of ~10 (to a few thousand) while the number of known BL Lac objects amounts to only ~110-140, barely twice the number discussed in Pittsburgh. What few complete, flux-limited samples do exist are very small, making statistical studies very difficult.

Nonetheless, considerable advances in our understanding of BL Lac objects have been made during the past ten years. It has become clear that relativistic beaming is a good explanation for the BL Lac phenomenon, accounting for rapid variability, high polarization, and the Compton catastrophe, provided that one can successfully explain the physics of jet formation, collimation, propagation, energetics, etc. The obvious question then becomes, what are the unbeamed (parent) objects? What do they look like when pointed away from the line of sight and how many of them are there? Is there a population consistent in unbeamed properties *and* in numbers with the known BL Lac population?

The effect of relativistic beaming on observed intensity is dramatic. The flux observed from a rapidly moving source can be orders of magnitude higher than the flux emitted in the rest-frame (*i.e.*, the flux that would be observed if the source were at rest with respect to the observer): $F_{obs} = \delta^p F_{intr}$, where $\delta = [\gamma(1-\beta\cos\theta)]^{-1}$ is the kinematic Doppler factor corresponding to velocity βc at an angle θ to the line of sight and $p = 3+\alpha$ for comparisons of flux density and a power law spectrum with index α. For a Lorentz factor $\gamma = 5$, sources with $\theta \lesssim 35°$ will have Doppler factors in the range 1-10, and for a reasonable spectral index ($\alpha \sim 1$), their apparent brightness will be enhanced by as much as 10^4. Therefore, if beaming is what makes BL Lac objects look like BL Lac objects, the consequences for population statistics are very severe.

Estimates of the volume density required for the parent population have been made by a number of authors. Some have tried to compensate for the effects of beaming (Schwartz and Ku 1983, Browne 1983, Perez-Fournon and Biermann 1984) while others use unbeamed luminosity (*e.g.*, host galaxy magnitude or large-scale symmetric radio luminosity) as a fiducial comparison between parents and BL Lacs (see papers by Browne and by Ostriker, this volume). The latter approach, while certainly correct, cannot be used for any flux-limited sample because it ignores the selection bias introduced by beaming. (One can still argue, as did Ostriker in his talk, that there are too few bright elliptical galaxies to hide the unbeamed BL Lacs; see discussion section at the end of this paper.) Because we are interested in well-defined, flux-limited samples, we concern ourselves here with the total (beamed plus unbeamed) luminosity.

Those papers that did consider the effects of beaming dealt with volume density integrated over luminosity, thereby missing the important aspect that the luminosity distribution of beamed objects is different from the parent distribution (Urry and Shafer 1984). In fact, for a single power law parent LF, the beamed LF is a broken power law, extremely flat at low luminosities and steepening to the parent slope at high luminosities. The derivation of this result is described briefly in §2.

The ratio of volume densities is therefore a function of luminosity. One cannot make meaningful numerical comparisons between parents and beamed objects without knowing the shape of both [observed] LFs. The full, intrinsic redshift distributions of parents and BL Lacs are obviously the same, so in any flux-limited sample the ratio of beamed objects to parents depends on where the luminosity distributions intersect. The effect is more important for steeper parent LFs because the slope of the beamed LF at low luminosities is always flat (it depends only on the strength of the beaming).

When Urry and Shafer (1984) first derived this result, the hope was that the luminosity function of BL Lac objects could be compared to the luminosity functions of potential parent populations. Unfortunately, the available estimates of BL Lac LFs (Véron 1979, Schwartz and Ku 1983, Urry 1984, Maccacaro *et al.* 1984), which we discuss in §3, are really only lower bounds to the true LF because the samples are not well-defined and redshift information is badly incomplete. The observed LF slopes are apparently very flat but whether this is due to beaming or to incompleteness is impossible to know.

A more promising approach is to look at the log*N*-log*S* (number counts versus flux) distribution for a completely identified, flux-limited sample. This has the advantage of not requiring redshift information, although partial redshift distributions provide an additional constraint on the underlying LF.

Recent X-ray results indicate that the log$N$-log$S$ distribution for BL Lac objects is unusually flat (see Maccacaro *et al.*, this conference), flatter than Euclidean, and much much flatter than the quasar distribution. In §4 we show briefly how a flat LF can lead directly to a flat log$N$-log$S$. In the near future we plan to fit the recently available radio and X-ray counts using a beamed LF. With the added constraint of partial redshift information, we should be able to put useful constraints on the parent luminosity function.

2. The Observed LF Derived from Beaming a Parent LF

2.1 Jets Randomly Oriented on the Sky

Suppose we have a parent population of relativistic jets with a known intrinsic luminosity function, $\phi(l)$, where l is the luminosity emitted isotropically in the rest frame of the jet. Now let the jets be randomly oriented on the sky so that only a few are pointing toward us. Of course these (which we call "beamed") will have greatly enhanced intensities and will be preferentially detected with respect to those jets pointing away (which we call "unbeamed"). To find the relative numbers of beamed and unbeamed sources seen, we derive the observed luminosity function, $\Phi(L)$, where $L = \delta^p l$ is the observed luminosity, δ is the Doppler factor defined earlier, and the exact value of p (~3-5) depends on the shape of the emitted spectrum and a number of other factors (whether l refers to monochromatic luminosity or luminosity integrated over a fixed bandwidth, whether injection or reacceleration of electrons occurs in a synchrotron source, etc.). For the present calculation (described in greater detail by Urry and Shafer 1984) we assume that all jets have the same relativistic velocity so that δ depends only on θ. The random distribution of angles on the sky then translates directly into a probability of observing a given value of the Doppler factor:

$$P(\delta) = (\beta\gamma\delta^2)^{-1} \quad , \tag{1}$$

assuming jets are two-sided. For a fixed jet luminosity l, the probability of observing luminosity L is

$$P(L \mid l) = P(\delta)\frac{d\delta}{dL} = \frac{1}{\beta\gamma p}\, l^{1/p} L^{-(p+1)/p} \quad . \tag{2}$$

For any differential parent LF $\phi(l)$, the observed LF will be

$$\Phi(L) = \int dl\, \phi(l)\, P(L \mid l) \quad . \tag{3}$$

As an example, consider a delta-function intrinsic LF, *i.e.* all jets have emitted, rest-frame luminosity l_0. The observed luminosity function of all beamed jets will simply follow the probability distribution of Equation 2, a power law in observed luminosity L with slope $(p+1)/p$. Figure 1 shows the integral LF, $L \times \Phi(L)$, normalized to the fiducial luminosity l_0 and to the total number of parent jets. It looks like a very flat incline — and the integral slope is only 0-0.5 for a wide range of values for p — with abrupt upper and lower cutoffs that depend on δ. The upper cutoff is the highest luminosity to which jets can be beamed, $L_{max} = \delta^p_{max}\, l_0$ where $\delta_{max} = \delta(0°) \approx 2\gamma$. (The value used in Fig. 1 is $\gamma = 5$.) Other jets are beamed away and so have reduced observed luminosities, between l_0 and $L_{min} = \delta^p_{min}\, l_0$, where $\delta_{min} \equiv \delta(90°) \approx \gamma^{-1}$. If we restrict our attention to those beamed jets whose intensity is Doppler boosted (*i.e.* those at angles $\theta < \theta_c$ where $\delta(\theta_c) \equiv 1$), then the observed LF lies between l_0 and $\delta^p_{max}\, l_0$ (the dashed line in Fig. 1).

If the intrinsic LF is instead a simple power law between l_1 and l_2,

$$\phi(l) = \begin{cases} K\, l^{-\beta}\,, & l_1 \le l \le l_2 \\ 0 \quad\;\, , & l < l_1 \text{ or } l > l_2 \end{cases} \quad , \tag{4}$$

the integral in Equation 3 can still be done analytically (with careful attention to the limits of integration; see Urry and Shafer 1984). The result is a broken power law LF for the beamed objects, flat at the low-luminosity end, steepening to the original (intrinsic) power law slope above luminosity $\delta_{max}^{p} l_1$ (Fig. 2a). This is easy to visualize as the superposition of the flat trapezoids in Figure 1. Again, we can separate the beamed population into two parts, those with $\theta < \theta_c$ (enhanced intensity) and $\theta > \theta_c$ (diminished intensity). This result is shown in Figure 2b for an intrinsic differential LF slope of $\beta = 2.75$ and for the same jet parameters as before ($\gamma = 5$ and $p = 4$).

2.2 Jets plus Isotropic, Unbeamed Component

The calculation we just did is unrealistic because one does not expect to find isolated jets. Radio interferometric maps of jets generally show some additional component that is approximately symmetric, often brighter, and presumably isotropic and unbeamed. In order to account for the contribution of the unbeamed component (l_u) to the total observed luminosity (L_T), we assume the intrinsic jet luminosity (l_j) is some fraction f of the unbeamed luminosity:

$$L_T = l_u + L_j = l_u + \delta^p l_j = l_u + \delta^p f l_u = (1 + f\,\delta^p) l_u \quad . \tag{5}$$

The conditional probability function $P(L_T \mid l_u)$ can now be derived from $P(\delta)$ (Eqn. 1) as before:

$$P(L_T \mid l_u) = \frac{1}{\beta\gamma p} f^{1/p}\, l_u^{-1} \left[\frac{L_T}{l_u} - 1 \right]^{-(p+1)/p} \quad . \tag{6}$$

The integral is now done numerically and the results are shown in Figure 3 (using the same jet and LF parameters as in Fig. 2). The assumed intrinsic luminosity function (solid line) is indistinguishable from the intrinsic LF assumed in the calculation because only a small fraction of the parent objects are beamed into a small-angle cone about the line of sight. The dashed lines represent the LFs of the jet-dominated objects, by which we mean $L_j > l_u$. In other words, the critical angle separating "beamed" from "unbeamed" objects is where $f\,\delta^p = 1$. Each dashed line in Figure 3 corresponds to a different value of the jet fraction: $f = 0.001$, 0.01, 0.1, or 1.0. Of course, the critical angle $\theta_c = \cos^{-1}[\beta^{-1}(1 - \gamma^{-1} f^{1/p})]$ is different for each of these values and the number of jet-dominated objects increases as f increases.

Figure 3 represents the expected LF for BL Lac objects (in the beaming picture) when the parent LF is a simple power law with sharp cutoffs. In the next section we discuss possible complications introduced by more realistic assumptions about the jet properties and parent LF but for the moment let us examine the important features of the beamed LF. First, the observed BL Lac LF has to be flatter than the observed LF for the parent objects. Second, the relative numbers observed depend on the lowest luminosity that is observable, (in effect the flux limit of each sample, given that the redshift distributions are necessarily the same). Third, most of the observed BL Lac objects will actually be the lowest luminosity parent objects. If the inevitable low luminosity turnover in the parent LF is not seen in current data, *then the bulk of the observed BL Lacs are inherently parent objects have not even been seen,* much less studied. This may make detailed comparisons — say of radio morphology, host galaxy characteristics, or polarization properties — very tricky.

2.3 Effects of More Complicated LF/ Beaming Models

We made several simplifying assumptions in calculating the luminosity functions in Figure 3. Almost certainly the real picture is more complicated but we already have a lot of free parameters (γ,

f, β, l_1, and l_2, although the last three are constrained by the parent LF and so depend only on which parent population is under consideration). As pointed out in the Introduction, the luminosity functions of BL Lac objects are anything but well-determined. Therefore we confine ourselves here to a qualitative discussion of how various likely refinements to the calculation will affect the observed, beamed LF.

First, the assumption that all jets move at the same velocity is clearly too simple. (Indeed, though too little is known about the physics of the jets, the jet velocity is probably not even constant within a single jet. However, emission at a given frequency may come from a restricted part of the jet that has an approximately constant velocity so fixing γ for each jet is less of a problem.) Suppose that there is a distribution of velocities among jets. It is easy to show that this has the effect of smoothing the sharp break in the beamed LF. Basically, as γ increases, the plateau in the LF grows longer (the break moves toward higher luminosity) and the overall normalization is reduced, as shown in Figure 4. Convolving the θ distribution with the γ distribution would effectively mean adding different amounts of the three curves in Figure 4, and the result would resemble their envelope. The LF would still be extremely flat at the low luminosity end, but at higher luminosities there would be a gradual steepening rather than a sharp break.

A more serious objection to our simple model in §2.2 is that the low-luminosity cutoff in the parent LF is unlikely to be as sharp as we assumed. Again, specifying a more gradual cutoff would add more free parameters and is only reasonable when a specific (*i.e.* observed) parent LF is involved. However, referring to Figure 1 it is easy to understand the effect of a gradual low-luminosity rollover in the parent LF. It can be approximated by a series of delta functions ($\delta(l-l_i)$) below some l_*. Then the observed LF of beamed sources is a series of trapezoids from l_i to $\delta^p_{max} l_i$, each with slope $(p+1)/p$ (as in Fig. 1). Below $\delta^p_{max} l_*$ the beamed LF would still have a differential slope $(p+1)/p$ (unless $\beta<(p+1)/p$, in which case it would have slope β below l_*) and would connect smoothly to the beamed LF calculated for a sharp cutoff (Fig. 2b). Thus the qualitative effect of a gradual rollover in the parent LF is negligible — the low-luminosity slope of the beamed LF is still very flat. Quantitatively it does matter a lot, since (1) beamed objects are dominated by the lowest luminosity parents, and (2) the ratio of beamed to unbeamed objects in a sample depends on the observed LF of both populations.

3. Estimates of X-Ray and Optical Luminosity Functions of BL Lac Objects

For reasons enumerated earlier, deriving an accurate luminosity function for BL Lac objects is currently impossible — there are no complete samples with enough redshift information. There do exist complete samples (*e.g.*, Maccacaro *et al.* and Stickel *et al.*, these proceedings) which, when redshifts are fully measured, will permit the derivation of X-ray and radio luminosity functions. In the meantime we have made some crude estimates of the optical and X-ray luminosity functions based on currently available information. These may, and probably do, suffer horribly from incompleteness and selection biases (BL Lacs being hard to find and redshifts being hard to measure), and so should not be taken as a measure of the true LF. Instead, they are lower limits to the true LF that represent the true shape of the LF only if the BL Lacs with known redshifts are drawn in an unbiased way from the full BL Lac population. (Since many redshifts come from absorption features in the host galaxy, the samples used here may in fact be strongly biased toward low z.)

We use a number of different techniques to estimate the BL Lac LFs. The details of the calculations are too lengthy to describe here (see Urry 1984 for more details) but our approaches include the following:

(1) The V/V_{max} method of Schmidt (1968), which is appropriate for complete, flux-limited samples. To derive the X-ray LF, we use the very small X-ray sample (~ 5-6 objects) of Piccinotti *et al.* (1982), which has a known flux limit. For the optical LF, we assume a *de facto* flux limit,

following Véron (1979) but with a larger sample (basically all BL Lacs with known redshifts, excluding the few high-redshift objects).

(2) A method described by Sramek and Weedman (1978) which uses the envelope of the z-L distribution. This was used by Schwartz and Ku (1983) in their estimate of the X-ray LF of BL Lac objects; we use additional redshift information and we apply the method to our optical sample as well.

(3) A new method in which, using only low-redshift objects (most BL Lacs have low redshifts in any case), we *require* $V/V_{max} \equiv 1/2$. This has the advantage that one need not specify a flux limit, and extensive tests on other samples shows that it is an adequate estimator of the LF in the absence of evolution (Urry 1984). This is done for both X-ray and optical samples of as many BL Lac objects as have measured [low] redshifts.

The resulting luminosity functions are shown in Figure 5. The most obvious characteristic is that, as found by Véron (1979) and Schwartz and Ku (1983), the LFs are quite flat. For both X-ray and optical luminosity functions, the integral slope is ~1 (with considerable uncertainty) and is distinctly flatter at the low-luminosity end. (This could obviously occur if we are missing the low-luminosity objects for some reason. In the beaming model, these are the objects in which the unbeamed luminosity is comparable to or greater than the beamed luminosity, possibly masking their BL Lac-ness in a self-consistent way. Therefore this is a serious problem.) For whatever reason, the LFs in Figure 5 are certainly flatter than is characteristic of other AGN like Seyfert galaxies and quasars, which tend to have integral slopes ≥2. Thus the estimates in Figure 5 are interesting, and certainly do not contradict the beaming model, but until better samples are available, we cannot say more.

4. The Relation Between Luminosity Functions and Number Counts

The analyses above are hampered largely by the lack of distance information, without which the luminosity and the volume of space probed are not known. Since fewer than one-third of the ~100 known BL Lac objects have measured redshifts, we really should work in number-flux space. Complete samples do give information about the number counts: $\log N$-$\log S$ curves for BL Lacs have recently been derived from the Medium Sensitivity Survey (Stocke *et al.* 1988, and Maccacaro *et al.*, this meeting), and they are remarkably flat — much, much flatter than the corresponding counts for quasars, and flatter even than the Euclidean slope of $-5/2$. The same appears to be true of optical samples although they are less well defined (Woltjer and Setti 1982). This can occur when the slope of the underlying luminosity function is very flat.

Briefly, we describe the relation between luminosity function and $\log N$-$\log S$. (There is a nice discussion of this by Shafer 1983.) Consider a uniform distribution of sources in infinite Euclidean space. The number of sources in a shell at distance r is

$$dN \approx \int_{L_{min}}^{L_{max}} \Phi(L)\, dL \;\; 4\pi r^2 dr \quad . \tag{7}$$

Now, since $r = (\frac{L}{4\pi S})^{1/2}$, we can express this in terms of flux through a change of variable:

$$dN = \left[\frac{1}{4\sqrt{\pi}} \int_{L_{min}}^{L_{max}} L^{3/2}\, \Phi(L)\, dL \right] S^{-5/2} dS \quad . \tag{8}$$

The quantity in brackets is just a normalization (depending on the number of objects) and so Equation 8 gives the familiar "Euclidean law". Independent of the exact form of the luminosity function, the differential source counts will have slope $-5/2$ as long as the source distribution is uniform throughout infinite space.

The counts are not Euclidean if the source distribution is not uniform. For example, sources can evolve. If their space density or average luminosity were higher in the past, then in general the counts steepen. This is why $\log N$-$\log S$ is usually steeper than Euclidean for quasars. It is important to note, however, that evolution produces less change in the counts when the slope of the luminosity function is flat (Cavaliere *et al.* 1983). Indeed the counts do not evolve at all when $\beta=1$ (Cavaliere, Giallongo, and Vagnetti 1986).

The slope of the number counts also changes when the volume over which sources are distributed is finite. Let r_{max} be the distance to the edge of the spherical volume in which sources are distributed. There are two fluxes at which the finiteness of space would become apparent: $S' \equiv \frac{L_{max}}{4\pi r_{max}^2}$, the flux at which the most luminous object is at the furthest distance; and $S_{min} \equiv \frac{L_{min}}{4\pi r_{max}^2}$, the smallest observable flux, corresponding to the least luminous source at the furthest distance. In qualitative terms, the effect of a spatial limit, r_{max}, is easy to see from Equation 8. For a LF with differential slope 2.5, the integral is proportional to L^{-1} and diverges logarithmically at both luminosity limits. For a steeper LF the low luminosity sources dominate, and so S_{min} is the flux at which the finiteness is manifested in the counts. That is, the counts will have a Euclidean slope down to the lowest flux (S_{min}) and then turn over abruptly. However, for a flatter LF the high luminosity objects dominate and S' is where the counts begin to flatten. In fact, it is easy to show that for a LF with slope $\beta < 2.5$ and $L_{max} >> L_{min}$, the slope of $\log N$-$\log S$ for $S < S'$ is β down to S_{min}, where the counts must roll over completely.

Therefore, for a flat luminosity function and a finite volume over which BL Lac objects are distributed, the counts flatten at relatively high fluxes, just as is observed. This is nearly equivalent to saying that flat counts imply negative evolution: either BL Lacs werer dimmer in the past or there were fewer of them (a redshift cutoff). The flat luminosity function is required by beaming, as we showed above; the finite volume could be a consequence of the relatively local distribution of the parent population (*e.g.* Fanaroff-Riley type I radio galaxies). Qualitatively, the agreement is excellent. Some preliminary work done in collaboration with Paolo Padovani after the Como conference suggests that we can match both the number counts and the redshift distribution with a simple beaming model and no evolution. The following detailed calculation remains to be done: starting with the luminosity function of FRI galaxies, beaming some fraction of their total radio luminosity, then predicting the counts of beamed objects and fitting the observed $\log N$-$\log S$ and $N(z)$. (Some spectral assumptions will have to go into the conversion between radio and X-ray bands.)

5. Conclusions and Summary

We showed that relativistic beaming leads naturally (and inexorably) to a flat LF, at least at the low luminosity end, independent of the form of the parent LF. The shapes of the parent LF and the beamed LF *will* be different, so that simply comparing ratios of volume densities (integrated over luminosity) is not an appropriate way to test the beaming hypothesis. (Even if one uses unbeamed luminosity as a fiducial, selection effects will enhance the number of beamed objects and thus will potentially distort even the unbeamed properties of the sample.) Furthermore, the prediction of a flat LF is consistent with existing estimates of the BL Lac LF (Véron 1979, Schwartz and Ku 1983, Urry 1984, and present paper), although such estimates are fraught with uncertainty. Much more reliable are the observed number counts, which are very flat (Woltjer and Setti 1982, Maccacaro *et al.* 1984); we showed that these can follow directly from a flat luminosity function and a finite spatial distribution. The observed counts (and partial redshift distribution) are qualitatively consistent with a model of

BL Lac objects as beamed versions of local ($z \leq 0.5$) low-luminosity radio galaxies, or as beamed versions of any parent population that does not evolve.

Acknowledgements — I would like to thank the organizers of the Como meeting, most especially Laura Maraschi, for arranging such a stimulating, useful, and very pleasant gathering at the Villa Olmo — may we all meet again under such agreeable circumstances in 1998. I am grateful to NASA for partial support of this work under the IUE program (grant NAG5-1034).

References

Browne, I. W. A. 1983, *M.N.R.A.S.*, **204**, 31p.

Burbidge, G., and Hewitt, A. 1987, *A. J.*, **92**, 1.

Cavaliere, A., Giallongo, E., Messina, A., and Vagnetti, F. 1983, in *Quasars and Gravitational Lenses*, ed. J. P. Swings, (Liège: Institut d'Astrophysique), p. 282.

Cavaliere, A., Giallongo, E., and Vagnetti, F. 1986, *Astr. Ap.*, **156**, 33.

Maccacaro, T., Gioia, I., Maccagni, D., and Stocke, J. 1984, *Ap. J. (Letter)*, **284**, L23.

Perez-Fournon, I. and Biermann, P. *Astr. Ap. (Letters)*, **130**, L13.

Piccinotti, G., Mushotzky, R.F., Boldt, E.A., Holt, S.S., Marshall, F.E., Serlemitsos, P.J., and Shafer, R.A. 1982, *Ap. J.*, **253**, 485.

Schmidt, M. 1968, *Ap. J.*, **151**, 393.

Schwartz, D. A., and Ku, W. H.-M. 1983, *Ap. J.*, **266**, 459.

Shafer, R. A. 1983, Ph. D. Thesis, University of Maryland.

Sramek, R. A., and Weedman, D. W. 1978, *Ap. J.*, **221**, 468.

Stocke, J. T., Morris, S. L., Gioia, I. M., Maccacaro, T., Schild, R.E., and Wolter, A. 1988, in *Proceedings of the Tucson Workshop on Optical Surveys for Quasars*, eds. P. S. Osmer, A. C. Porter, R. F. Green, and C. B. Foltz, *Astr. Soc. Pac. Conf. Series*, **2**, 311.

Urry, C.M. 1984, Ph.D. Thesis, The Johns Hopkins University.

Urry, C. M., and Shafer, R. A. 1984, *Ap. J.*, **280**, 569.

Véron, P. 1979, *Astr. Ap.*, **78**, 46.

Woltjer, L., and Setti, G. 1982, *Astrophysical Cosmology*, eds. H. A. Brück, G. V. Coyne, and M. S. Longair, Pont. Acad. Scientiarum Scripta Varia, **48**, 293.

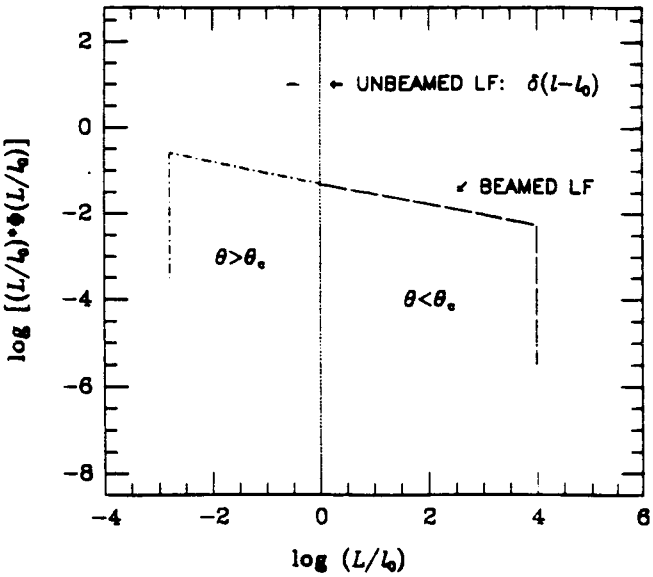

Figure 1. The observed luminosity function when all jets have intrinsic luminosity l_0. Luminosities are normalized to l_0 and the ordinate is the integral LF $L/l_0 \times \Phi(L/l_0)$, normalized to the total number of jets (*i.e.* the integral of the plotted function is 1). For this Figure we used $\gamma=5$ and $p=4$, and for these parameters $\theta_c=35.3°$.

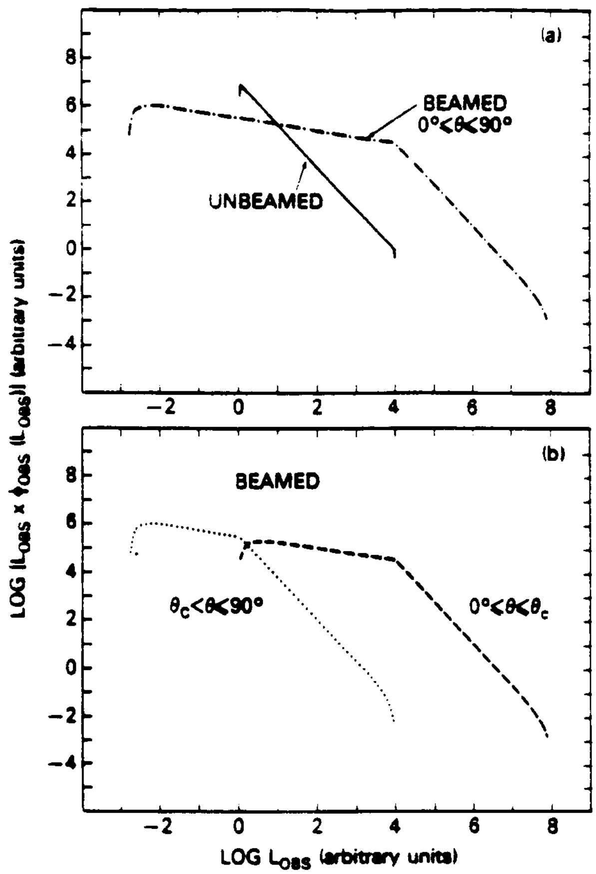

Figure 2. The observed luminosity function when jets have an intrinsic power-law LF (solid line) with differential slope $\beta=2.75$ and sharp upper and lower cutoffs (Eqn. 4). The beamed LF (all angles) is the dot-dash line in panel (a); the beamed LF separated where $\delta=1$ is shown in panel (b). As before, $\gamma=5$, $p=4$, and $\theta_c=35.3°$.

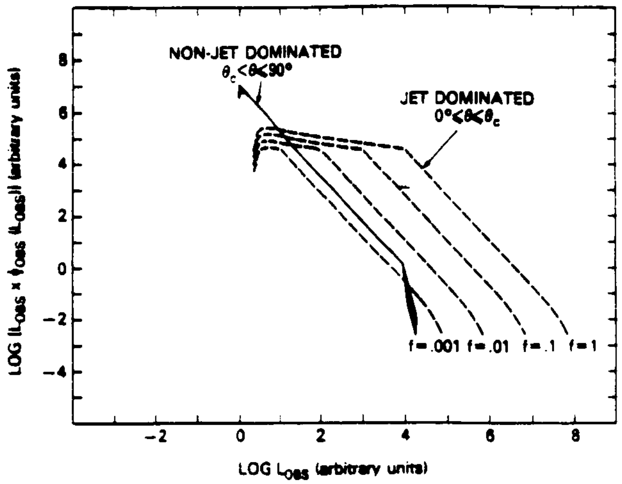

Figure 3. Total luminosity functions for jet-dominated (BL Lac) objects and non-jet-dominated (parent) objects when the parent luminosity consists of a beamed jet plus an unbeamed, isotropic component. The intrinsic jet luminosity is assumed to be a fixed fraction f of the unbeamed luminosity, and the beamed LFs for four different values of f are plotted (dashed lines). The solid line represents the non-jet-dominated LFs; on this scale these LFs for different f are indistinguishable from one another or from the intrinsic LF assumed. In contrast to Figs. 1 and 2, the critical angle θ_c is now defined as the angle for which the observed jet and unbeamed luminosities are equal. Obviously more and more objects appear beamed (because θ_c increases) as the fraction f increases.

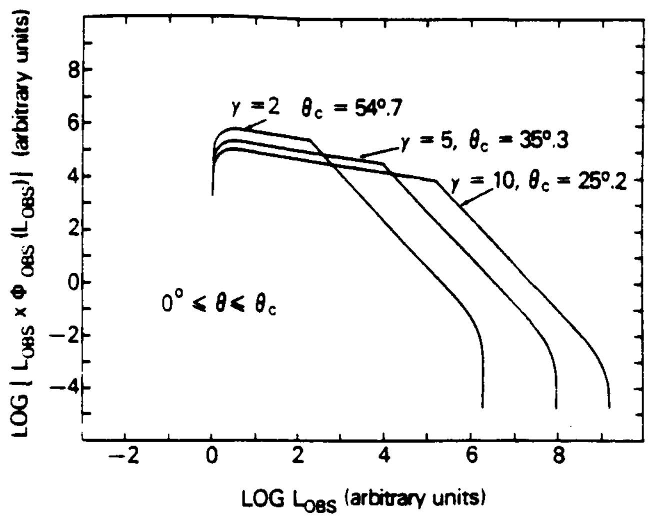

Figure 4. The effect of jet Lorentz factor γ on the observed beamed luminosity function. The three curves represent observed integral beamed LFs derived from a single-component (jets only) parent LF (β=2.75 and p=4) using three different values of Lorentz factor: γ=2, 5, and 10. Note that the critical angle decreases with increasing γ, so fewer beamed objects are expected for high jet velocities; however, at high luminosities they vastly outnumber the beamed objects with low-velocity jets.

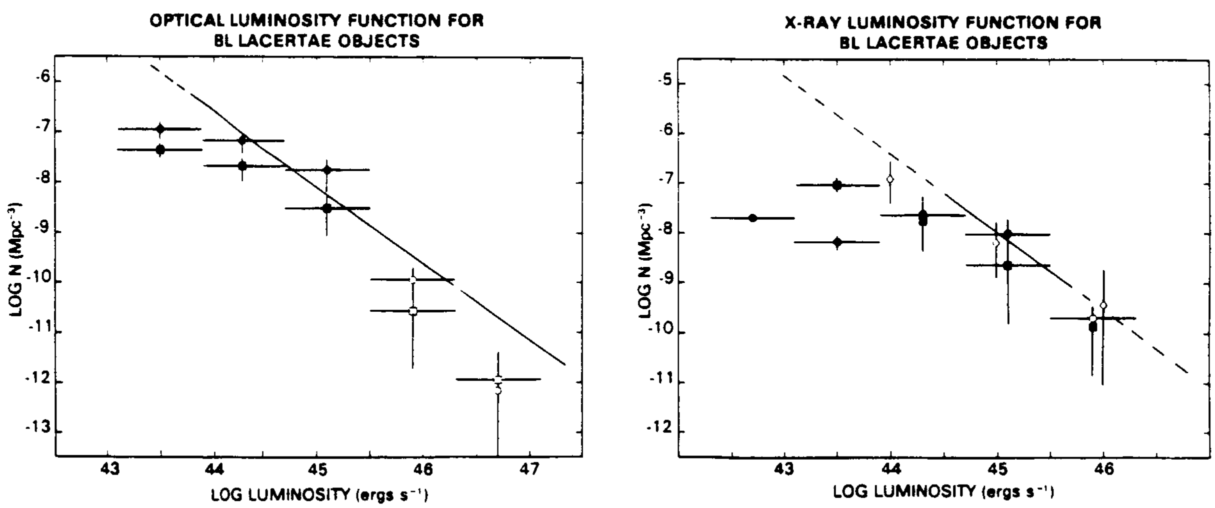

Figure 5. Estimated luminosity functions for known BL Lac objects with redshifts. The methods and samples were discussed in detail by Urry (1984); newer calculations using the same techniques but the somewhat different BL Lac catalog of Burbidge and Hewitt (1987) are not perceptibly different, especially given the large uncertainties.

(a) Optical LF. *Squares* — V/V_{max} method of Schmidt (1968) for 13 local (z< 0.07) objects (solid squares) and 20 nearby (z< 0.4) objects (open squares). *Circles* — V_{max}= 2 method for the same two samples. *Line* — Envelope method of Sramek and Weedman (1978). The solid line represents the luminosity range for which the envelope is defined; the dashed line is an extrapolation.

(b) X-ray LF. Symbols are the same as above except as noted. *Shaded squares* — Five objects from the Piccinotti *et al.* (1982) sample, with no correction for incompleteness. *Open diamonds* — results of Schwartz and Ku (1983), derived from a similar sample (compare to solid line).

QUESTIONS

J. Ostriker: The beaming will bring up to detectability faint and relatively more common objects but it does not affect the host galaxy. Thus we are forced to multiply the number of BL Lac host objects by a factor of 10^4 for beaming with additional corrections for incompleteness, etc. You may exceed the density of local radio giant ellipticals.

M. Urry: Yes, I should have said explicitly in my talk that both you and Ian Browne used unbeamed power (host galaxy brightness and extended radio power, respectively) to do the population statistics, in which case the method outlined here is not relevant. (Of course, for well-defined, flux-limited samples, it *is* necessary since one is then looking at the total [beamed plus unbeamed] flux.) Now, if every BL Lac is in the most luminous giant elliptical galaxy and it is beamed with $\gamma \sim 23$ (for $\theta \sim 1/\gamma \sim 2.5°$), as you suggested in your talk, then I agree there may indeed be a problem.

T. Maccacaro: Which kind of redshift distribution do you predict from integration of your best luminosity function?

M. Urry: I have not done this yet because prior to this meeting there was no well-determined $\log N$-$\log S$ to fit and of course there are many free parameters (*e.g.*, parent luminosity function, Lorentz factor of the jet, fraction of unbeamed luminosity in the jet, etc.). Now that you and also Paolo Giommi have reported a detailed $\log N$-$\log S$ from X-ray flux-limited samples, it becomes an important exercise. Your talk suggested that it will be hard to produce the observed redshift distribution without a cutoff at $z \sim 0.5$ — it will be interesting to see if this changes materially because of the two-power-law luminosity function or, even better, to see if we can do it self-consistently, taking the redshift distribution and luminosity function of a suggested parent population like the FRI galaxies, beaming some fraction of the luminosity at random angles on the sky, and producing an observed $\log N$-$\log S$ and $N(z)$ that match what you and Giommi and Stickel observe. Obviously this is a strong test of the beaming model. (Note added several months after the meeting: Paolo Padovani and I have done some preliminary work on this project, and we think it will not be difficult to produce the observed flat counts and apparent redshift cutoff at $z \sim 0.5$ with a beamed luminosity function and no evolution in the parent population.)

B. Wills: As I mentioned before (after the Maccacaro and Stocke talks), the optical synchrotron component may have a very steep spectrum so when one defines the sample by optical characteristics, these objects may be missing at high redshift, *i.e.* at short rest wavelengths, where the synchrotron component is weak.

M. Urry: This effect is accounted for in our picture (it appears as the α in the exponent of the boosting factor, $\delta^{3+\alpha}$, which we parametrize more simply as δ^p) as long as the spectrum is a single power law over the full spectral range of interest, *i.e.* for observations at frequency ν_0, the power law must extend from ν_0/δ to $\nu_0(1+z)/\delta$, where $1 \le \delta \le \delta_{max}$. If the spectrum is curved, then additional selection effects are of course present.